Desalination 311 (2013) 95–102

Contents lists available at SciVerse ScienceDirect

Desalination

journal homepage: www.elsevier.com/locate/desal

An application of the Sano–Nakayama membrane transport model in hollow fiber reverse osmosis desalination systems

Akira Nakayama [a,b,*], Yoshihiko Sano [a]

[a] Dept. of Mechanical Engineering, Shizuoka University, 3-5-1 Johoku, Naka-ku, Hamamatsu, 432-8561 Japan
[b] School of Civil Engineering and Architecture, Wuhan Polytechnic University, Wuhan, Hubei 430023, China

HIGHLIGHTS

- A novel membrane transport model is proposed for reverse osmosis modules.
- All governing equations are combined into three ordinary differential equations.
- One can estimate all characteristics analytically without appealing to FDM.
- The present analysis agrees well with available experimental data.
- The model can be used to design efficient radial flow reverse osmosis modules.

ARTICLE INFO

Article history:
Received 23 February 2012
Received in revised form 11 November 2012
Accepted 13 November 2012
Available online 20 December 2012

Keywords:
Reverse osmosis
Hollow fiber module
Porous media
Mathematical model

ABSTRACT

The Sano–Nakayama membrane transport model recently proposed for the analysis of a countercurrent dialyzer system has been extended to describe the concentration polarization phenomena associated with hollow fiber reverse osmosis desalination systems. A set of the governing equations, namely, the continuity, momentum and concentration equations, is derived for three distinctive phases, namely, brine, permeate and membrane phases, exploiting a volume averaging approach. These equations based on the Sano–Nakayama model are coupled and subsequently reduced to three distinctive first-order ordinary equations in terms of the average velocity, pressure and salt concentration of the brine phase. These equations along with an algebraic equation for the permeate flow rate per unit volume can readily be solved to estimate permeate salinity, permeate flow rate and pressure drop in a hollow fiber reverse osmosis desalination system. Available experimental data and numerical results based on finite difference methods are found to agree well with the present analytical estimates based on the Sano–Nakayama model.

1. Introduction

Reverse osmosis is being widely practiced for water purification. Hollow fiber reverse osmosis modules are most extensively used for both domestic and industrial water purification, since they provide high specific surface area and recovery factor. Various membrane transport models are available for mathematically describing transport phenomena through membranes with concentration polarization. Among them, the resistance-in-series models e.g. [1,2] have been widely used for speedy practical estimations, in which the polarization resistance is introduced empirically to be added to the membrane resistance. Kimura and Sourirajan [3] introduced the solution–diffusion in which the membrane is assumed to be impermeable to a solute. The solute accumulates on the membrane surface resulting in concentration polarization. This model, which accounts for the polarization often disregarded, was adopted by many researchers including Gupta [4,5], Ohya et al. [6], Evangelista and Jonsson [7] and Tweddle et al. [8]. Gupta [4,5] employed this solution–diffusion model to investigate tubular, plate-and-frame and spiral modules [4] as well as radial flow hollow fiber modules [5]. Ohya et al. [6] verified his mathematical model based on the solution–diffusion model using their own experimental data.

Sekino [9,10] proposed the friction–concentration–polarization model based on the solution–diffusion model so as to consider the polarization as well as the pressure drops within both brine and permeate phases. Radial flow hollow fiber modules were considered solving a set of differential equations by a finite difference method [9,10]. Subsequently, his model was adopted by Al-Bastaki and Abbas [11,12], Kumano et al. [13] and Marcovecchio et al. [14] for estimating desalination performance of actual modules. Chatterjee et al. [15] extended Sekino's friction–concentration–polarization model, replacing the solution–diffusion model by the three-parameter, non-linear, Spiegler–Kedem model [16], and then resorted to a finite difference method to analyze the performances of radial flow hollow fiber reverse osmosis modules. In the Spiegler–Kedem model, the so-called reflection

* Corresponding author at: Dept. of Mechanical Engineering, Shizuoka University 3-5-1 Johoku, Hamamatsu, 432-8561 Japan.
E-mail address: tmanaka@ipc.shizuoka.ac.jp (A. Nakayama).

0011-9164/$ – see front matter © 2012 Elsevier B.V. All rights reserved.
http://dx.doi.org/10.1016/j.desal.2012.11.012

coefficient is introduced as another parameter in addition to two parameters commonly used in the solution–diffusion model, namely, hydrodynamic permeability and solute permeability. The Spiegler–Kedem model is believed to be more accurate for describing transport phenomena through membranes with polarization, as demonstrated by Murthy and Gupta [17,18].

In this study, it will be shown that the Sano–Nakayama membrane transport model originally introduced for the analysis of dialyzer system [19] is readily applicable for describing transport processes through membranes with concentration polarization. The model based on a volume averaging theory is quite simple, yet, will be proven to be as accurate as the Spiegler–Kedem model. Thus, the set of the governing equations, namely, the continuity, momentum and solute concentration equations for the brine, permeate and membrane, readily reduce to three distinctive first-order ordinary equations in terms of the average velocity, pressure and salt concentration of the brine phase. These equations along with an algebraic equation for the permeate flow rate per unit volume may easily be solved to estimate permeate salinity, flow rate and pressure drop in hollow fiber reverse osmosis modules. Available experimental data and numerical results based on finite difference methods are found to agree well with the present estimates based on the Sano–Nakayama model. The mathematical model presented here will be quite useful for analytically designing an efficient radial flow hollow fiber reverse osmosis desalination system, without resorting to extensive finite difference calculations.

2. Mathematical model

A radial flow hollow fiber reverse osmosis module is illustrated in Fig. 1, in which the fibers are packed in the module. The fibers may be in parallel to or wound around the feeder core tube, in which the feed stream enters. The fiber bores are sealed at one end and open at the other such that the permeate can flow out axially to be collected. The concentrated brine, on the other hand, flows out radially outwards to be collected at the outer side of the fiber bundle, as indicated in the figure.

The concentration polarization takes place within the membrane, as illustrated in Fig. 2, so that the solute concentration in the membrane surface at the shell side remains higher than those of brine (reject) and permeate streams. In all previous analyses, certain membrane transport models such as the solution–diffusion model and Spiegler–Kedem model are introduced to characterize the mass transfer through the membrane. Thus, some relationships between the concentration of the polarized membrane surface and those of the brine and permeate

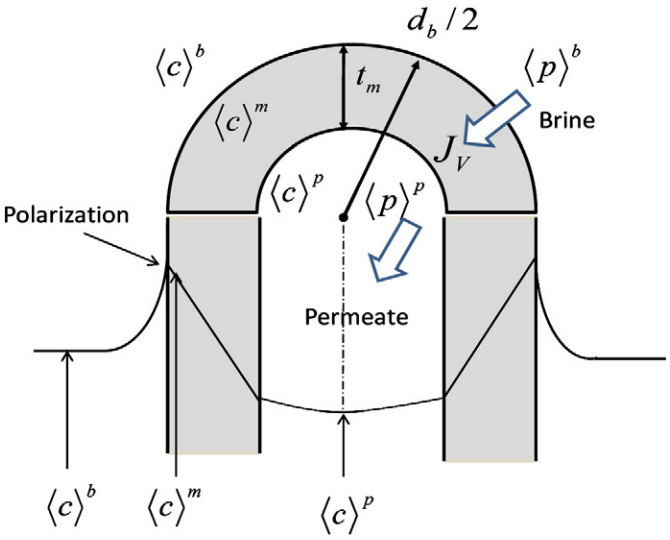

Fig. 2. Concentration polarization in the membrane surface.

are prescribed in advance, with the help of the membrane parameters, such as hydrodynamic permeability, solute permeability and reflection coefficient.

Sano and Nakayama [19] on the other hand introduced a porous media approach based on the local volume averaging theory [20,21] and considered all mass and momentum conservation equations for three individual phases, namely, the shell side fluid, lumen side fluid and membrane phases, in the study of countercurrent hemodialyzer systems. They derived the relationships among three individual concentrations, without introducing a priori membrane transport model. The resulting Sano–Nakayama membrane transport model is found to follow the Kedem–Katchalsky model [22] closely. In this study, the same approach as introduced by Sano and Nakayama is extended to derive the desalination version of the Sano–Nakayama membrane transport model, and then to investigate the concentration polarization phenomena associated with hollow fiber reverse osmosis desalination systems.

Sano and Nakayama [19] considered the governing equations, namely, the continuity, momentum and species mass transfer equations, for the three individual phases, namely, the shell side fluid, lumen side fluid and membrane phases, and integrated them over a local control volume. The resulting set of the volume averaged governing equations

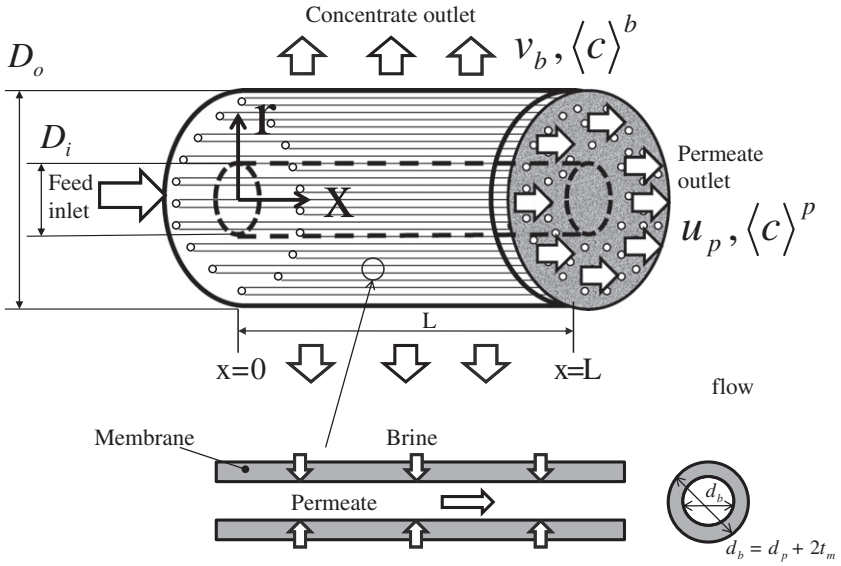

Fig. 1. Radial flow hollow fiber reverse osmosis module.

have been closed by means of modeling the unknown terms associated with subscales in terms of the volume averaged quantities (i.e. the dependent variables). The steady state assumption is valid when the time scale for the temporal variation of the average feed pressure is sufficiently large as compared with the residence time of the fluid, namely, $\pi\left(D_0{}^2-D_i{}^2\right)L/4Q_{feed}$, which is of the order 10 to 100 s for the present case. In most of hollow fiber reverse osmosis modules, this condition is satisfied, and the steady state (or quasi-steady state) assumption holds during most time of the operation. Thus, the set of the volume averaged governing equations may readily be translated for the present steady case of reverse osmosis desalination phenomena, as follows:

For the brine phase:

$$\frac{\partial \varepsilon_b \left\langle u_j \right\rangle^b}{\partial x_j} + \omega = 0 \tag{1}$$

$$\frac{\partial \langle p \rangle^b}{\partial x_i} = -\frac{\mu_b}{K_{b_{ij}}} \varepsilon_b \left\langle u_j \right\rangle^b - \varepsilon_b{}^2 \rho_b b_{bij} \sqrt{\langle u_k \rangle^b \langle u_k \rangle^b} \left\langle u_j \right\rangle^b \tag{2}$$

$$\frac{\partial \varepsilon_b \left\langle u_j \right\rangle^b \langle c \rangle^b}{\partial x_j} = -\omega \langle c \rangle^b - a_b h_b \left(\langle c \rangle^b - \langle c \rangle^m \right). \tag{3}$$

For the permeate phase:

$$\frac{\partial \varepsilon_p \left\langle u_j \right\rangle^p}{\partial x_j} - \omega = 0 \tag{4}$$

$$\frac{\partial \langle p \rangle^p}{\partial x_i} = -\frac{\mu_p}{K_{p_{ij}}} \varepsilon_p \left\langle u_j \right\rangle^p - \varepsilon_p{}^2 \rho_p b_{pij} \sqrt{\langle u_k \rangle^p \langle u_k \rangle^p} \left\langle u_j \right\rangle^p \tag{5}$$

$$\frac{\partial \varepsilon_p \left\langle u_j \right\rangle^p \langle c \rangle^p}{\partial x_j} = (1-\sigma)\omega \langle c \rangle^m - a_b h_m \left(\langle c \rangle^p - \langle c \rangle^m \right). \tag{6}$$

For the membrane phase:

$$\frac{\partial}{\partial x_j}\left(\varepsilon_m D_{m_{jk}} \frac{\partial \langle c \rangle^m}{\partial x_k} \right) + \omega \langle c \rangle^b + a_b h_b \left(\langle c \rangle^b - \langle c \rangle^m \right) - (1-\sigma)\omega \langle c \rangle^m + a_b h_m \left(\langle c \rangle^p - \langle c \rangle^m \right) = 0 \tag{7}$$

where

$$\omega = a_b J_v = \frac{1}{V} \int_{A_{b_{\text{int}}}} u_j n_{b_j} dA = a_b L_p \left\{ \left(\langle p \rangle^b - \langle p \rangle^p \right) - \sigma \frac{iR\langle T \rangle^m}{M} \left(\langle c \rangle^m - \langle c \rangle^p \right) \right\}. \tag{8}$$

Eqs. (1)–(3) describe the continuity, momentum and salt mass balance equations for the brine phase, while Eqs. (4)–(6) describe the continuity, momentum and salt mass balance equations for the permeate phase, respectively. These three-dimensional tensorial set of the macroscopic governing equations along with the salt mass balance Eq. (7) for the membrane phase may be used for full three-dimensional numerical calculations, as proposed for the case of the dialyzer system [19].

As for the operating conditions, the feed pressure, flow rate and salt concentration are given along with the pressure at the permeate outlet. The appropriate boundary conditions for the set of the foregoing partial differential equations may readily be generated from these feed values, as the geometrical configuration of the desalination module is provided.

The sub- and super-scripts b, p and m are assigned to the brine, permeate and membrane phases, respectively, such that a_b and a_p are the specific surface area of the brine (shell) side area (i.e. the total outer wall surface area of the hollow fibers per unit volume) and that of the permeate (lumen) side area (i.e. the total inner wall surface area of the hollow fibers per unit volume). Moreover, ε_b, ε_p and ε_m $(=1-\varepsilon_b-\varepsilon_p)$ are the volume fractions of the brine, permeate and membrane phases, respectively. As carrying out a volume averaging procedure, one decomposes a certain variable ϕ into its intrinsic average $\langle \varphi \rangle^f$ and spatial deviation $\tilde{\varphi}$:

$$\varphi = \langle \varphi \rangle^f + \tilde{\varphi} \tag{9}$$

where the intrinsic average $\langle \varphi \rangle^f$ is defined as

$$\langle \varphi \rangle^f = \frac{1}{V_f} \int_{V_f} \varphi dV. \tag{10}$$

The volume V_f ($f=b$, p, m) is the volume space, which f phase in question (brine, permeate or membrane) occupies within the total local control volume V. As defined in Eq. (8), $\omega \equiv \frac{1}{V}\int_{A_{b_{\text{int}}}} u_j n_{b_j} dA$ is the total permeate volume flow rate per unit volume (i.e. the permeate stream production rate per unit volume) which is the product of the specific area of the membrane surface a_b and the total permeate volume flux J_v through the membrane. As usual, the membrane is characterized in terms of three parameters, namely, the hydraulic permeability L_p, the solute permeability h_m and the reflection coefficient σ. Moreover, the osmotic pressure is given by $(iR\langle T \rangle^m/M)(\langle c \rangle^m - \langle c \rangle^p)$ where i $(=2)$, R $(=8341$ J/kg kmol K), M $(=58.3)$ and $\langle T \rangle^m$ are the number of ions for ionized solutes (i.e. Vant Hoff factor), ideal gas constant, molecular weight of solute and feed brine temperature, respectively. As closing the equations to obtain Eqs. (1)–(3), the surface integral terms over the membrane wall surface are modeled as follows:

$$\frac{1}{V_b}\int_{A_{b_{\text{int}}}} \left(\mu_b \frac{\partial u_i}{\partial x_j} - p\delta_{ij} \right) n_{bj} dA - \frac{\partial}{\partial x_j}\left(\rho \left\langle \tilde{u}_i \tilde{u}_j \right\rangle^b \right) = -\frac{\mu}{K_{b_{ij}}} \varepsilon_b \left\langle u_j \right\rangle^b - \varepsilon_b{}^2 \rho_b b_{bij} \sqrt{\langle u_k \rangle^b \langle u_k \rangle^b} \left\langle u_j \right\rangle \tag{11}$$

$$\frac{1}{V}\int_{A_{b_{\text{int}}}} c u_j n_{bj} dA = \omega \langle c \rangle^b \tag{12}$$

$$\frac{1}{V}\int_{A_{b_{\text{int}}}} D_b \frac{\partial c}{\partial x_j} n_{bj} dA = a_b h_b \left(\langle c \rangle^b - \langle c \rangle^m \right) \tag{13}$$

where n_{bi} is the unit vector pointing outward from the brine side to membrane side, while $A_{b\text{int}}$.is the interfacial area between the brine and membrane phases. A similar modeling procedure can be taken for the surface integral terms for the permeate phase to obtain Eqs. (4)–(6).

Only the difference between the present set of the governing equations and that of Sano and Nakayama [19] is the introduction of the reflection coefficient σ, which represents the rejection capability of a membrane (i.e., $\sigma=0$ for no rejection and $\sigma=1$ for perfect rejection). As one sets $\sigma=0$, the set of the equations naturally reduces to that of Sano and Nakayama originally proposed for the analysis of hemodialyzer systems.

3. Application of the Sano–Nakayama model to reverse osmosis desalination modules

The set of the equations based on the Sano–Nakayama model may be simplified further to investigate the concentration polarization phenomena associated with hollow fiber reverse osmosis modules. One notes that the macroscopic diffusion within the membrane is negligibly small as compared with the interfacial mass transfer terms since the hollow fibers are not consolidated. (Note that the ratio of the interfacial mass transfer to the mass diffusion in the membrane phase corresponds with the Sherwood number $h_m L/D_m$ which is usually much greater than

1.) Thus, the differential Eq. (7) reduces to an algebraic equation:

$$\omega\langle c\rangle^b + a_b h_b\left(\langle c\rangle^b - \langle c\rangle^m\right) - (1-\sigma)\omega\langle c\rangle^m + a_b h_m\left(\langle c\rangle^p - \langle c\rangle^m\right) = 0. \quad (14a)$$

The first two terms on the left hand side of the equation correspond with the salt coming from the brine side through the brine/membrane interface, while the last two terms correspond with the salt coming from the permeate side through the permeate/membrane interface. Note that the last two terms are negative, since the salt permeates through the membrane interface from the membrane side to permeate side. Eq. (14a) may be solved for $\langle c\rangle^m$ as

$$\langle c\rangle^m = \frac{(a_b h_b + \omega)\langle c\rangle^b + a_b h_m \langle c\rangle^p}{a_b h_b + a_b h_m + (1-\sigma)\omega}. \quad (14b)$$

The mass transfer coefficient h_b between the brine and membrane (i.e. shell side) may be estimated according to Sekino [9]:

$$\frac{h_b d_b}{D_b} = 0.048\left(\frac{\rho_b \varepsilon_b \left|\left\langle \vec{u}\right\rangle^b\right| d_b}{\mu_b}\right)^{0.6}\left(\frac{\mu_b}{\rho_b D_b}\right)^{1/3}. \quad (15)$$

The total mass transfer resistance between the membrane and permeate, on the other hand, is approximated by $1/a_b h_m$ as in Eq. (6), since the mass transfer coefficient between the permeate and membrane (i.e. lumen side) is much higher than the solute permeability of the membrane h_m:

$$\frac{1}{a_b h_m} + \frac{1}{a_p h_p} \cong \frac{1}{a_b h_m}. \quad (16)$$

In the radial flow hollow fiber reverse osmosis module, the volume averaged permeate flow velocities are aligned axially, while the volume averaged brine flow velocities are radially directed outwards from the core tube. Thus, one may assume these velocity vectors' components (u,v) as

$$\varepsilon_b\langle u_i\rangle^b = (0, v_b) \quad (17a)$$

and

$$\varepsilon_p\langle u_i\rangle^p = \left(u_p, 0\right) \quad (17b)$$

where v_b and u_p are the apparent radial flow velocity of the brine and the apparent axial flow velocity of the permeate, respectively. Thus, the macroscopic governing Eqs. (1)–(6) reduce to:

For the brine phase:

$$\frac{1}{r}\frac{\partial r v_b}{\partial r} = -\omega \quad (18)$$

$$\frac{\partial\langle p\rangle^b}{\partial r} = -\frac{150(1-\varepsilon_b)^2}{\varepsilon_b{}^3 d_b{}^2}\mu_b v_b - 1.75\frac{1-\varepsilon_b}{\varepsilon_b{}^3 d_b}\rho_b v_b{}^2 \quad (19)$$

$$\frac{1}{r}\frac{\partial r v_b\langle c\rangle^b}{\partial r} = -\omega\langle c\rangle^b - h_{bv}\left(\langle c\rangle^b - \langle c\rangle^m\right). \quad (20)$$

For the permeate phase:

$$\frac{\partial u_p}{\partial x} = \omega \quad (21)$$

$$\frac{\partial\langle p\rangle^p}{\partial x_i} = -\frac{32\mu_p}{\varepsilon_p d_p{}^2}u_p \quad (22)$$

$$\frac{\partial u_p\langle c\rangle^p}{\partial x} = (1-\sigma)\omega\langle c\rangle^m - h_{mv}\left(\langle c\rangle^p - \langle c\rangle^m\right) \quad (23)$$

where $h_{bv} = a_b h_b$ and $h_{mv} = a_b h_m$ are the volumetric mass transfer coefficients. The Hagen–Poiseuille permeate flow is assumed to prevail in the hollow fibers, while the radial brine flow through fibers is approximated by the flow through a porous medium, introducing the Ergun equation.

Noting $u_p(0,r) = 0$ at the closed end, Eq. (21) may be integrated as

$$u_p(x,r) = \int_0^x \omega dx = \bar{\omega}x \quad (24a)$$

such that

$$\bar{u}_p(r) = \frac{1}{2}\bar{\omega}L \quad (24b)$$

where

$$\bar{\varphi}(r) = \frac{1}{L}\int_0^L \varphi dx \quad (25)$$

is the value averaged over the module length L such that

$$\bar{\omega}(r) = a_b L_p\left\{\left(\overline{\langle p\rangle^b} - \overline{\langle p\rangle^p}\right) - \sigma\frac{iR\langle T\rangle^m}{M}\left(\overline{\langle c\rangle^m} - \overline{\langle c\rangle^p}\right)\right\}. \quad (26)$$

Noting $\langle p\rangle^p(L,r) = p_{atm}$ (i.e. atmospheric pressure) at the permeate outlet, Eq. (22) with Eq. (24a) yields

$$\langle p\rangle^p(x,r) = p_{atm} + \frac{32\mu_p}{2\varepsilon_p d_p{}^2}\bar{\omega}\left(L^2 - x^2\right) \quad (27a)$$

such that

$$\overline{\langle p\rangle^p}(r) = p_{atm} + \frac{32\mu_p}{3\varepsilon_p d_p{}^2}\bar{\omega}L^2. \quad (27b)$$

Then, one may integrate Eq. (23), noting Eq. (24a) and $u_p(0,r) = 0$, and find

$$\langle c\rangle^p(x,r) = \overline{\langle c\rangle^p}(r) = \frac{(1-\sigma)\bar{\omega}\overline{\langle c\rangle^m} - h_{mv}\left(\overline{\langle c\rangle^p} - \overline{\langle c\rangle^m}\right)}{\bar{\omega}} \quad (28a)$$

or

$$\overline{\langle c\rangle^p}(r) = \frac{(1-\sigma)\bar{\omega} + h_{mv}}{\bar{\omega} + h_{mv}}\overline{\langle c\rangle^m}. \quad (28b)$$

Thus, using Eqs. (28b) and (14b), one may express the concentration of the permeate $\overline{\langle c\rangle^p}$ and that of the polarized membrane $\overline{\langle c\rangle^m}$ in terms of the concentration of the brine $\langle c\rangle^b$ alone as

$$\overline{\langle c\rangle^p} = \frac{((1-\sigma)\bar{\omega} + h_{mv})(\bar{\omega} + h_{bv})}{(\bar{\omega} + h_{mv})(\bar{\omega} + h_{bv}) - \sigma\bar{\omega}^2}\overline{\langle c\rangle^b} \quad (29)$$

and

$$\overline{\langle c\rangle^m} = \frac{(\bar{\omega} + h_{mv})(\bar{\omega} + h_{bv})}{(\bar{\omega} + h_{mv})(\bar{\omega} + h_{bv}) - \sigma\bar{\omega}^2}\overline{\langle c\rangle^b}. \quad (30)$$

Eqs. (28b) and (29) readily give the intrinsic salt rejection $R_{in} = \left(\overline{\langle c\rangle^m} - \overline{\langle c\rangle^p}\right)/\overline{\langle c\rangle^m}$ and the solute concentration ratio $\overline{\langle c\rangle^p}/\overline{\langle c\rangle^b}$ as

$$R_{in} = \frac{\sigma}{1 + \frac{1}{(J_v/h_m)}} \quad (31a)$$

and

$$\frac{\langle c\rangle^p}{\langle c\rangle^b} = 1 - \frac{\frac{\sigma}{(J_v/h_b)}}{\left(1+\frac{1}{(J_v/h_b)}\right)\left(1+\frac{1}{(J_v/h_m)}\right)-\sigma} \tag{31b}$$

where the relations $\bar{\omega}/h_{bv} = J_v/h_b$ and $\bar{\omega}/h_{mv} \cong J_v/h_m$ are used. In Figs. 3 and 4, these results for the intrinsic rejection and solute concentration ratio (with $J_v/h_b = 0.1$) are compared against those of the Spiegler–Kedem model [16], which run as

$$R_{in} = \frac{\sigma(1-\exp(-(1-\sigma)(J_v/h_m)))}{1-\sigma\exp(-(1-\sigma)(J_v/h_m))} \tag{32a}$$

and

$$\frac{\langle c\rangle^p}{\langle c\rangle^b} = \frac{(1-\sigma)\exp(J_v/h_b)}{(1-\sigma)\exp(J_v/h_b)+\sigma(1-\exp(-(1-\sigma)(J_v/h_m)))}. \tag{32b}$$

The expressions (31a) and (31b) of the Sano–Nakayama model appear to be much simpler than those of the Spiegler–Kedem model (Eqs. (32a) and (32b)) which involves in exponential functions. The two models, despite the difference in their appearances, agree fairly well with each other. It is interesting to note that the membrane transport characteristics are automatically described in the present set of the governing equations. Thus, no additional membrane transport models are needed in the present approach.

Having derived the Sano–Nakayama model as given by Eqs. (29) and (30), Eqs. (18)–(20) for the brine are integrated from $x=0$ to $x=L$. Then, the foregoing Eqs. (24b), (27b), (29) and (30) are substituted into these integrated equations and Eq. (26), to obtain the following set of the equations written solely in terms of the brine phase quantities:

$$\frac{d\overline{v_b}}{dr} = -\frac{\overline{v_b}}{r} - \bar{\omega} \tag{33}$$

$$\frac{d\overline{\langle p\rangle^b}}{dr} = -\frac{150(1-\varepsilon_b)^2}{\varepsilon_b{}^3 d_b{}^2}\mu_b\overline{v_b} - 1.75\frac{1-\varepsilon_b}{\varepsilon_b{}^3 d_b}\rho_b\overline{v_b}^2 \tag{34}$$

$$\frac{d\overline{\langle c\rangle^b}}{dr} = \frac{\sigma\bar{\omega}^2 h_{bv}}{(\bar{\omega}+h_{mv})(\bar{\omega}+h_{bv})-\sigma\bar{\omega}^2}\frac{\overline{\langle c\rangle^b}}{\overline{v_b}} \tag{35}$$

where

$$\bar{\omega} = a_b L_p\left\{\left(\overline{\langle p\rangle^b} - p_{atm} - \frac{32\mu_p}{3\varepsilon_p d_p{}^2}\bar{\omega}L^{*2}\right) - \frac{iR\langle T\rangle^m}{M}\frac{\sigma^2\bar{\omega}(\bar{\omega}+h_{bv})}{(\bar{\omega}+h_{mv})(\bar{\omega}+h_{bv})-\sigma\bar{\omega}^2}\overline{\langle c\rangle^b}\right\} \tag{36}$$

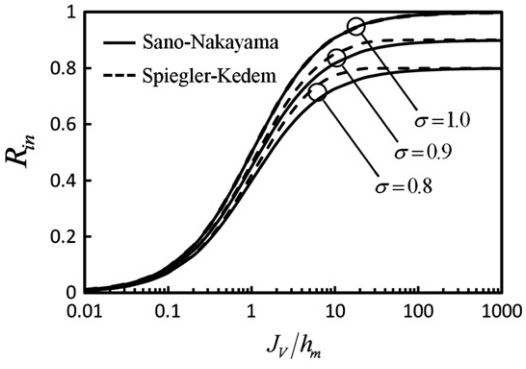

Fig. 3. Intrinsic salt rejection.

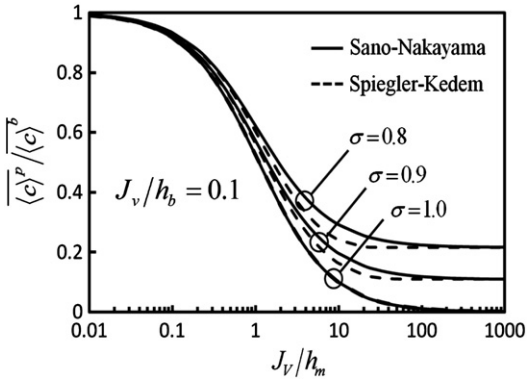

Fig. 4. Solute concentration ratio.

where

$$L^*(r) = \sqrt{L^2 + (2W\pi r)^2}$$

is the effective length of the hollow fibers which may be wound W times at the radius r. The first order ordinary differential Eqs. (33)–(35) with the algebraic Eq. (36) may readily be integrated to find $\overline{v_b}(r)$, $\overline{\langle p\rangle^b}(r)$ and $\overline{\langle c\rangle^b}(r)$, using any standard integration scheme such as the Runge–Kutta–Gill method (see e.g. Nakayama [23]). The algebraic Eq. (36) may be re-arranged to form a cubic equation for $\bar{\omega}$, which may readily be shot for a positive root. The boundary conditions at $r = D_i/2$ for the three first order differential equations are given by

$$\overline{v_b}|_{r=D_i/2} = \frac{Q_{feed}}{\pi D_i L},\ \overline{\langle p\rangle^b}\Big|_{r=D_i/2} = p_{feed},\ \overline{\langle c\rangle^b}\Big|_{r=D_i/2} = c_{feed}. \tag{37a, b, c}$$

One may integrate these equations to the end at $r = D_o/2$, to find the permeate production rate Q_p as

$$Q_p = Q_{feed} - \pi D_o L\overline{v_b}\Big|_{r=D_o/2}. \tag{38}$$

Subsequently, the bulk mean salt concentration of the permeate stream flowing out of the module, c_p, may be estimated from

$$c_p = \frac{Q_{feed}c_{feed} - \pi D_o L\overline{v_b}|_{r=D_o/2}\,\overline{\langle c\rangle^b}|_{r=D_o/2}}{Q_p}. \tag{39}$$

4. Results and discussion

Chatterjee et al. [15] and Sekino [9] numerically investigated reverse osmosis separation processes in Toyobo Hollosep modules, solving the set of the friction–concentration–polarization model equations written in the axi-symmetric coordinates by finite difference methods. Sekino [9] used the two-parameter solution–diffusion membrane model, whereas Chatterjee et al. [15] introduced the three-parameter Spiegler–Kedem membrane model. The specifications of Toyobo Hollosep module and its operating conditions are listed in Table 1.

The present analysis based on Eqs. (33)–(36) enables one to estimate the permeate salinity, permeate flow rate and recovery factor, without resorting to exhaustive finite difference calculations. In Fig. 5, such estimates on the permeate flow rate Q_p and the ratio of the concentrations of the produced permeate to the feed brine, c_p/c_{feed} are presented against the feed brine flow rate Q_{feed} for the case of Toyobo Hollosep module, $c_{feed} = 35$ kg/m^3 and $p_{feed} = 5.5$ MPa, with the other specifications as listed in Table 1. The reflection coefficient σ is set to 0.9 and 0.95 to show the effects of rejection capability of a membrane on Q_p and c_p/c_{feed}. The present results agree well with the finite

Table 1
Specifications of Toyobo Hollosep module and its operating conditions.

d_b	163×10^{-6} m
d_p	70×10^{-6} m
L_p	2.73×10^{-13} m/s Pa
h_m	8.12×10^{-10} m/s
ε_b	0.45
$\varepsilon_p=\varepsilon_b(d_p/d_b)^2$	0.083
D_i	0.04 m
D_o	0.19 m
L	0.99 m
S	361 m^2
$a_b\cong a_p=4S/\pi\left(D_o{}^2-D_i{}^2\right)L$	1.35×10^4/m
W	2
σ	0.9–1.0
Q_{feed}	$2–25\times10^{-4}$ m^3/s
c_{feed}	30–45 kg/m^3 (35kg/m^3)
p_{feed}	5.0–6.5 MPa (5.5 MPa)
p_{atm}	0.1 MPa
$\langle T\rangle^m$	298 K
ρ_b	1060 kg/m^3
μ_b	1.09×10^{-3} Pa s
μ_p	0.90×10^{-3} Pa s
D_b	5.0×10^{-9} m^2/s
R	8341 J/kg kmol K
M	58.3
i	2
$h_b=\frac{0.048D_b}{d_b}\left(\frac{\rho_b v_b d_b}{\mu_b}\right)^{0.6}\left(\frac{\mu_b}{\rho_b D_b}\right)^{1/3}$, $L^*(r)=\sqrt{L^2+(2W\pi r)^2}$	

difference calculation results obtained by Chatterjee et al. [15] with Spiegler–Kedem model.

The radial developments of the variables $\overline{v_b}(r)$, $\overline{\langle p\rangle^b}(r)$, $\overline{\langle c\rangle^b}(r)$ and $\bar{\omega}(r)$ for the case of $\sigma=0.9$, $Q_{feed}=15\text{x}10^{-4}$ m^3/s, $c_{feed}=35$ kg/m^3 and $p_{feed}=5.5$ MPa are presented in Fig. 6(a) and (b). The radial velocity of the brine decreases from 0.0121 m/s to 0.002 m/s as the pressure drops by 0.075 atmospheric pressure towards the outlet. The permeate volume flow rate per unit volume ω (i.e. the permeate production rate per unit volume) decreases only slightly from 0.0097/m to 0.0072/m, while the rejected salt concentration of the brine increases from 35.0 kg/m^3 to 40.4 kg/m^3, indicating both effective salt rejection and uniform production of the permeate within the whole module.

Sekino [9] reported various sets of experimental data obtained using the afore-mentioned Toyobo Hollosep module. He investigated the individual effects of c_{feed}, p_{feed} and the recovery factor $Rc\equiv Q_p/Q_{feed}$ on Q_p and c_p/c_{feed}. The present analytical results with $\sigma=1$ are compared against his experimental data in Fig. 7(a) to (c), which show reasonable agreement with the experimental data. The results for fixed Rc were obtained iteratively to find the boundary value Q_{feed} which yields $Q_p=RcQ_{feed}$. Thus, one can readily and accurately estimate all transport characteristics associated with radial flow hollow fiber reverse osmosis modules, simply by solving Eqs. (33)–(36) for given specifications.

5. Conclusions

It has been shown that the Sano–Nakayama membrane transport model originally introduced for the analysis of countercurrent hemodialyzer system is able to describe transport processes through membranes with concentration polarization, as observed in hollow fiber reverse osmosis desalination systems. The volume averaged governing equations based on the Sano–Nakayama membrane transport model were integrated to form three distinctive first-order ordinary equations in terms of the average velocity, pressure and salt concentration of the brine phase. The equations along with an algebraic equation for the permeate volume flow rate per unit volume were solved to find permeate salinity, permeate flow rate and pressure drops in a hollow fiber reverse osmosis module. The results are found to agree well with the finite difference calculation results of Chatterjee et al. as well as the experimental data of Sekino. The present model can be used to design an efficient radial flow hollow fiber reverse osmosis desalination system, without resorting to extensive finite difference calculations.

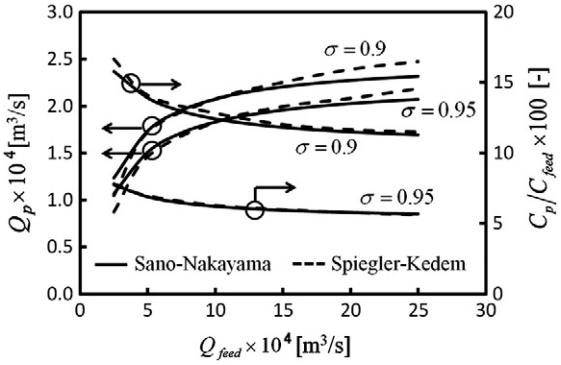

Fig. 5. Variations of permeate variables with feed brine flow rate.

Nomenclature

A_{int}	interface between the fluid and membrane phases [m^2]
$a_{b,p}$	specific surface area [1/m]
$b_{b,p}$	Forchheimer coefficient [1/m]
c	salt concentration [kg/m^3]
c_p	bulk mean salt concentration of the permeate flowing out of the module
$d_{b,p}$	inner and outer diameters of the hollow fiber [m]
$D_{i,o}$	inner and outer diameters of the fiber bundle [m]
D_b	diffusivity of the brine [m^2/s]
h_b	mass transfer coefficient of the brine (shell side) [m/s]
h_m	solute permeability of the membrane [m/s]

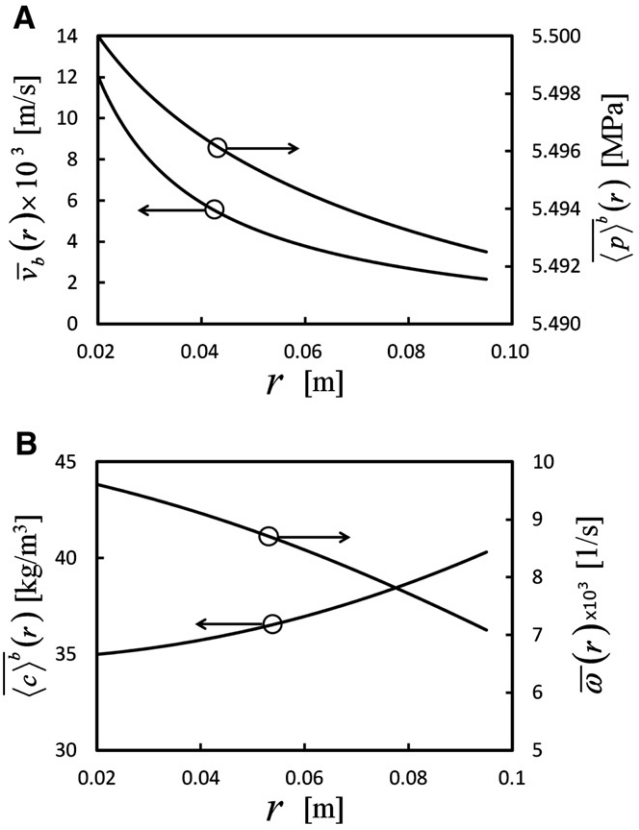

Fig. 6. Radial variations of brine variables. ($\sigma=0.9$, $Q_{feed}=15\times10^{-4}$ m^3/s, $c_{feed}=35$ kg/m^3 $p_{feed}=5.5$ MPa). (a)Velocity and pressure (b) Concentration and permeate production rate per unit volume.

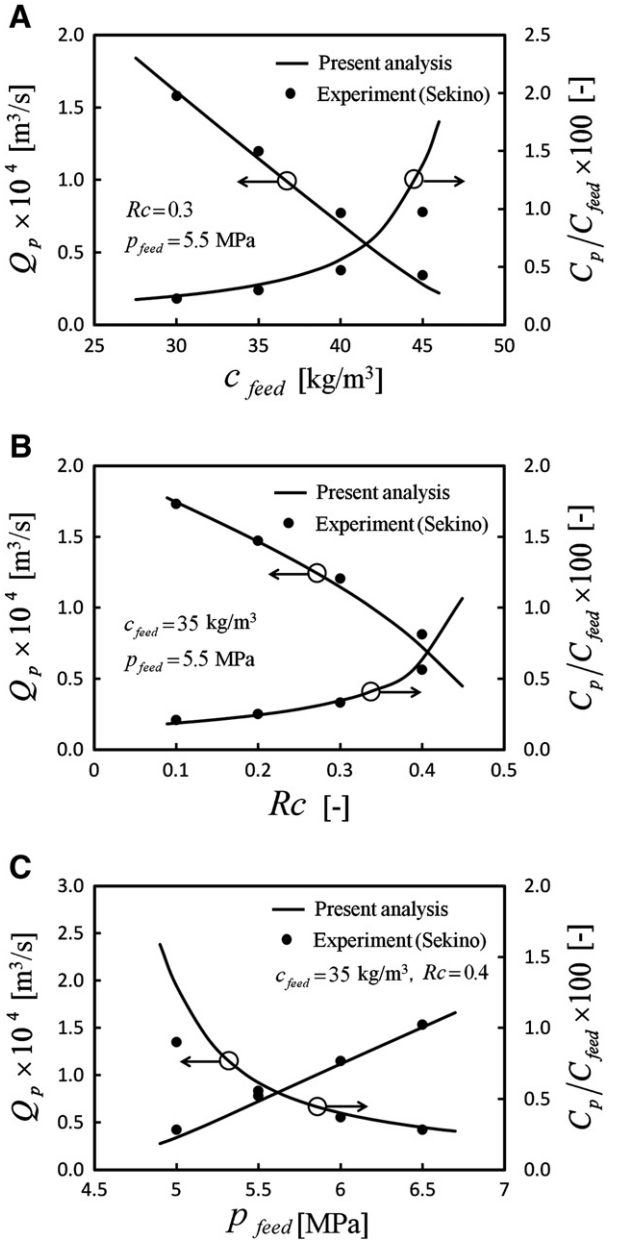

Fig. 7. Comparison between the present analysis and Sekino's experimental data. (a) Effects of c_{feed} on Q_p and c_p/c_{feed} (b) Effects of Rc on Q_p and c_p/c_{feed}. (c) Effects of p_{feed} on Q_p and c_p/c_{feed}.

i	Vant Hoff factor
J_V	permeate volume flux through the membrane [m/s]
$K_{b,p}$	permeability [m^2]
L	effective length of the module [m]
L_p	hydraulic permeability of the membrane [m/s Pa]
M	molecular weight of the solute [−]
n_i	unit vector pointing outward from the fluid side to membrane side [−]
p	pressure [Pa]
Q_{feed}	feed brine flow rate [m^3/s]
Q_p	permeate flow rate [m^3/s]
r	radial coordinate [m]
R	universal gas constant [J/kg kmol K]
R_{in}	intrinsic rejection [−]
Rc	recovery
S	total membrane surface area [m^2]
t_m	membrane thickness [m]
$\langle T\rangle^m$	temperature of the feed brine [K]
v_b	Dacian velocity of the brine [m/s]
u_p	Dacian velocity of the permeate [m/s]
u_i	velocity vector [m/s]
V	representative elementary volume [m^3]
W	number of wound of hollow fibers [−]
x	axial coordinate [m]

Greek symbols

$\varepsilon_{b,p,m}$	volume fraction [−]
μ	viscosity [Pa s]
ρ	density [kg/m3]
σ	reflection coefficient [−]
ω	permeate volume flow rate per unit volume [1/s]

Special symbols

$\tilde{\varphi}$	deviation from intrinsic average
$\langle\varphi\rangle^{b,p,m}$	intrinsic average

Subscripts and superscripts

b	brine
p	permeate
m	membrane
$feed$	feed brine

References

[1] I. Borsi, O. Lorain, A space-averaged model for hollow fiber membranes filters, Comput. Chem. Eng. 39 (2012) 65–74.
[2] A.F. Derradji, S. Taha, G. Dorange, Application of the resistances in series model in ultrafiltration, Desalination 184 (2005) 377–384.
[3] S. Kimura, S. Sourirajan, Analysis of data in reverse osmosis with porous cellulose acetate membranes, AICHE J. 13 (1967) 497–503.
[4] S.K. Gupta, Analytical design equations for reverse osmosis systems, Ind. Eng. Chem. Process. Des. Dev. 24 (1985) 1240–1244.
[5] S.K. Gupta, Design and analysis of a radial-flow hollow-fiber reverse-osmosis system, Ind. Eng. Chem. Res. 26 (1987) 2319–2323.
[6] H. Ohya, H. Nakajima, K. Takagi, S. Kagawa, Y. Negishi, An analysis of reverse osmotic characteristics of B-9 hollow fiber module, Desalination 21 (1977) 257–274.
[7] F. Evangelista, G. Jonsson, Explicit design of hollow fiber reverse osmosis systems, in: Proceedings of ICOM, 2, 1990, pp. 1081–1085.
[8] T.A. Tweddle, W.L. Thayer, T. Matsuura, H. Fu-Hung, Specification of commercial reverse osmosis modules and predictability of their performance for water treatment applications, Desalination 32 (1980) 181–198.
[9] M. Sekino, Precise analytical model of hollow fiber reverse osmosis module, J. Membr. Sci. 85 (1993) 241–252.
[10] M. Sekino, Study of an analytical model for hollow fiber reverse osmosis module systems, Desalination 100 (1995) 85–97.
[11] N.M. Al-Bastaki, A. Abbas, Modeling an industrial reverse osmosis unit, Desalination 126 (1999) 33–39.
[12] N.M. Al-Bastaki, A. Abbas, Predicting the performance of RO membranes, Desalination 132 (2000) 181–187.
[13] A. Kumano, M. Sekino, Y. Matsui, N. Fujiwara, N. Fujiwara, Study of mass transfer characteristics for a hollow fiber reverse osmosis module, J. Membr. Sci. 324 (2008) 136–141.
[14] M.G. Marcovecchio, N.J. Scenna, P.A. Aguirre, Improvements of a hollow fiber reverse osmosis desalination model: analysis of numerical results, Chem. Eng. Res. Des. 88 (2010) 789–802.
[15] A. Chatterjee, A. Ahluwalia, S. Senthilmurugan, S.K. Gupta, Modeling of a radial flow hollow fiber module and estimation of model parameters using numerical techniques, J. Membr. Sci. 236 (2004) 1–16.
[16] K.S. Spiegler, O. Kedem, Thermodynamics of hyperfiltration (reverse osmosis): criteria for efficient membranes, Desalination 1 (1966) 311–326.
[17] Z.V.P. Murthy, S.K. Gupta, Sodium cyanide separation and parameter estimation for reverse osmosis thin film composite polyamide membrane, J. Membr. Sci. 154 (1994) 89–103.
[18] Z.V.P. Murthy, S.K. Gupta, Thin film composite polyamide membrane parameters estimation for phenol–water system by reverse osmosis, Sep. Sci. Technol. 33 (1998) 2541–2557.
[19] Y. Sano, A. Nakayama, A porous media approach for analyzing a countercurrent dialyzer system, ASME Trans. J. Heat Transfer 134 (7) (2012) 072602.

[20] A. Nakayama, F. Kuwahara, A general bioheat transfer model based on the theory of porous media, Int. J. Heat Mass Transfer 51 (2007) 3190–3199.
[21] A. Nakayama, F. Kuwahara, Y. Kodama, An equation for thermal dispersion flux transport and its mathematical modelling for heat and fluid flow in a porous medium, J. Fluid Mech. 563 (2006) 81–96.
[22] O. Kedem, A. Katchalsky, Thermodynamics analysis of the permeability of biological membranes to non-electrolytes, Biochim. Biophys. Acta 27 (1958) 229–246.
[23] A. Nakayama, in: PC-aided Numerical Heat Transfer and Convective Flow, CRC Press, Boca Raton, 1995, pp. 17–21.